

Breast Reconstruction with Deep Inferior Epigastric Artery Perforator Flap: 3.0-T Gadolinium-enhanced MR Imaging for Preoperative Localization of Abdominal Wall Perforators¹

Victoria Chernyak, MD
Alla M. Rozenblit, MD
David T. Greenspun, MD
Joshua L. Levine, MD
David L. Milikow, MD
Frank A. Chia, MD
Heather A. Erhard, MD

Purpose:

To prospectively evaluate 3.0-T gadolinium-enhanced magnetic resonance (MR) imaging for localization of inferior epigastric artery (IEA) perforators before reconstructive breast surgery involving a deep inferior epigastric perforator (DIEP) flap.

Materials and Methods:

This study was exempt from institutional review board approval, and the requirement for informed patient consent was waived. Data were collected and stored in compliance with HIPAA regulations. Nineteen patients (mean age, 46.3 years) underwent three-dimensional gadolinium-enhanced 3.0-T MR imaging of the abdomen before undergoing DIEP flap breast reconstruction. Up to four of the largest perforators arising from the IEA on each side of the umbilicus were identified. The diameter, intramuscular course, and distance from the umbilicus of each perforator were recorded. One of the marked perforators on each side was labeled “the best” on the basis of an optimal combination of perforator features: diameter, intramuscular course, and location with respect to the flap edges. MR findings were compared with intraoperative findings. The two-tailed Student *t* test was used to compare the mean diameters of all perforators with the mean diameters of the perforators labeled as the best.

Results:

There were 30 surgical flaps, and 11 (58%) of the 19 patients underwent bilateral flap dissection. At surgery, 122 perforators were localized, and 118 (97%) of these perforators—with a mean diameter of 1.1 mm (range, 0.8–1.6 mm)—had been identified at preoperative MR imaging. Thirty perforators with a mean diameter of 1.4 mm (range, 1.0–1.6 mm) were labeled as the best at MR imaging. Thirty-three perforators were harvested intraoperatively, and all of these had been localized preoperatively. Twenty-eight (85%) of these 33 perforators were labeled as the best at MR imaging.

Conclusion:

Gadolinium-enhanced 3.0-T MR imaging can be used to accurately localize IEA perforators and to select the optimal perforator to be harvested for DIEP flap reconstructive breast surgery.

© RSNA, 2008

¹ From the Departments of Radiology (V.C., A.M.R., D.L.M., F.A.C.) and Plastic Surgery (H.A.E.), Montefiore Medical Center, 111 E 210th St, Bronx, NY 10467; David T. Greenspun, MD, MSc, New York, NY (D.T.G.); and The Center for Microsurgical Breast Reconstruction of Manhattan and Charleston, New York, NY (J.L.L.). Received February 29, 2008; revision requested April 30; revision received June 17; accepted July 2; final version accepted July 23. Address correspondence to V.C. (e-mail: vichka17@hotmail.com).

Reconstructive breast surgery after mastectomy remains a common treatment option for some patients with breast cancer. Traditionally, it has been performed by using pedicled flaps such as transverse rectus abdominis myocutaneous (TRAM) flaps (1). During the TRAM flap procedure, the surgeon harvests a portion of rectus muscle and overlying subcutaneous fat and uses these tissues to reconstruct the breast. A segment of the inferior epigastric artery (IEA) harvested along with the flap is anastomosed to the internal mammary artery to provide a blood supply to the reconstructed breast.

An alternative microsurgical breast reconstruction technique called deep inferior epigastric perforator (DIEP) flap reconstruction was developed recently. During this procedure, the breast is reconstructed by using the subcutaneous abdominal fat only, leaving the underlying rectus muscle intact. The area of the flap is centered around the umbilicus (Fig 1). During the course of the surgery, the surgeon dissects the fat off the rectus fascia. To create a blood supply for the flap, the surgeon meticulously dissects the area of the flap, dissecting unnamed small branches that arise from the IEA (1). These branches, usually called perforators, course through the rectus muscle and extend into the sub-

cutaneous fat. Ideally, a single best perforator is harvested (1). The decision of which perforator to harvest is based on the size and location of the vessel; ideally, a single dominant perforator in the center of the flap is taken (1). Once a perforator is selected, it is dissected through the rectus muscle down to the IEA; then, a portion of the IEA as well as a perforator are harvested (Fig 1). In bilateral breast reconstruction, the perforators on both sides of the umbilicus are identified, whereas in unilateral reconstruction, the perforators on the side contralateral to the mastectomy site are harvested.

The DIEP flap has certain advantages over the TRAM flap: It is associated with lower rates of donor site complications, such as pain, abdominal wall laxity or hernia, and functional impairment, and often yields a better cosmetic appearance (1). However, the DIEP flap procedure involves a much longer dissection time because the location of the perforators is variable and the entire area of the flap has to be dissected to locate perforators that are often 1 mm in diameter or smaller. In the TRAM flap procedure, no preoperative imaging is necessary because the location of the IEA is fairly predictable.

The standard examination for preoperative localization of the perforators for DIEP flap reconstructive surgery is Doppler ultrasonography (US) (2). Although preoperative Doppler US can provide an overall view of the distribution of the individual perforators, it is

associated with a high rate of false-positive results and a considerable rate of false-negative results (3). For DIEP flap breast reconstruction, preoperative cross-sectional imaging evaluation has been reported to be highly beneficial (2,4,5). Alonso-Burgos et al (4) and Masia et al (5) found that preoperative knowledge of the location and diameters of the perforators facilitated shorter dissection times and greater ability to plan the location of the flap. In both these studies, four- and 16-detector computed tomography (CT) was evaluated and shown to be highly accurate for preoperative localization of the perforators (4,5). However, because DIEP flap surgery is a cosmetic procedure, one can assume that a younger subgroup of breast cancer patients would seek it; therefore, the exposure to ionizing radiation associated with the use of CT may be an important drawback. The purpose of our study was to evaluate 3.0-T gadolinium-enhanced MR imaging for localization of IEA perforators before DIEP flap reconstructive breast surgery, which would obviate the patient's exposure to radiation.

Advances in Knowledge

- A three-dimensional (3D) gadolinium-enhanced T1-weighted fat-suppressed gradient-echo sequence performed by using a 3.0-T MR imager was used to localize 97% of the perforating arteries arising from the inferior epigastric artery (IEA) before deep inferior epigastric artery perforator (DIEP) flap reconstructive breast surgery.
- T1-weighted 3D fat-suppressed gradient-echo gadolinium-enhanced MR imaging was used to predict with 85% accuracy which perforator arising from the IEA would be the most favorable to harvest for DIEP flap breast reconstruction.

Implications for Patient Care

- The described 3D gadolinium-enhanced T1-weighted fat-suppressed gradient-echo sequence performed at 3.0 T yields an accurate map of the location of anterior abdominal wall perforators before DIEP flap breast reconstruction and thus facilitates intraoperative localization of these small vessels.
- By performing MR imaging, one can avoid exposing this relatively young subgroup of breast cancer patients to ionizing radiation.

Materials and Methods

The authors had no financial interests in any products, drugs, or devices associated with this study. There were no commercial interests, such as stock

Published online before print

10.1148/radiol.2501080307

Radiology 2009; 250:417-424

Abbreviations:

DIEP = deep inferior epigastric perforator
IEA = inferior epigastric artery
3D = three-dimensional
TRAM = transverse rectus abdominis myocutaneous

Author contributions:

Guarantors of integrity of entire study, V.C., A.M.R.; study concepts/study design or data acquisition or data analysis/interpretation, all authors; manuscript drafting or manuscript revision for important intellectual content, all authors; manuscript final version approval, all authors; literature research, V.C., D.G.; clinical studies, all authors; statistical analysis, V.C.; and manuscript editing, V.C., A.M.R., D.M., F.A.C.

Authors stated no financial relationship to disclose.

ownership, consultancies, or patent licensing arrangements, that might have represented a conflict of interest with the information presented in this article.

Study Design

Our institutional review board exempted this study from approval, and the requirement for informed patient consent was waived. The data were collected and stored according to Health Insurance Portability and Accountability Act regulations. This study included patients scheduled to undergo elective DIEP flap breast reconstruction performed by the participating surgeons (D.T.G., J.L.L., H.A.E.). Patients who had any of the established contraindications to MR imaging or who declined to undergo MR imaging owing to marked claustrophobia were excluded from the study. We prospectively collected the data from MR imaging of the anterior abdominal wall performed in patients before they underwent DIEP flap reconstruction. All MR examinations were performed at one institution (Montefiore Medical Center) between September 2006 and August 2007.

Patients

A total of 21 women were scheduled to undergo DIEP flap breast reconstruction

during the specified period (between September 2006 and August 2007). One patient was excluded from MR imaging owing to the presence of a soft-tissue expander; another patient was excluded because she had marked claustrophobia. Thus, a total of 19 patients (mean age, 46.3 years; age range, 31–64 years) underwent preoperative MR imaging of the abdominal wall before undergoing DIEP flap breast reconstruction at our institution during the specified period. A total of 30 surgical flaps were used in the 19 patients: 11 (58%) patients (mean age, 47.3 years; range, 41–54 years) underwent bilateral flap dissection, and eight (42%) patients (mean age, 44.9 years; range, 31–64 years) underwent unilateral flap dissection. There was no significant difference in age between these two groups ($P = .52$).

MR Imaging

All examinations were performed by using a 3.0-T imager (Philips Achieva, software version 10.6; Philips Medical Systems, Best, the Netherlands) and an eight-channel torso surface coil. A three-dimensional (3D) gadolinium-enhanced fat-suppressed T1-weighted gradient-echo sequence—specifically, a T1-weighted high-resolution isotropic volume examination (THRIVE; Philips

Medical Systems)—was performed in the axial plane. The scanning delay was 20 seconds; three consecutive breath-hold acquisitions were performed. The parameters used for the MR acquisition are summarized in the Table. All patients received a standard dose (0.1 mmol per kilogram of body weight) of gadopentetate dimeglumine (Magnevist; Bayer Schering, Leverkusen, Germany) followed by 20 mL of normal saline solution at an injection rate of 2 mL/sec.

Image Interpretation

Each MR image was interpreted by one of two board-certified radiologists with 2 (V.C.) and 22 (A.M.R.) years of experience in abdominal imaging. A single radiologist reviewed the images obtained in all three gadolinium-enhanced acquisitions and determined those images that demonstrated the highest signal intensity of the perforators with the least venous contamination. These images were reviewed in detail by the same radiologist to determine the perforator location.

In each case, up to four of the largest perforators were localized on each side of the umbilicus for potential harvesting. The size (diameter, in millimeters) of the perforator and the distance of the perforator from the umbilicus

Figure 1

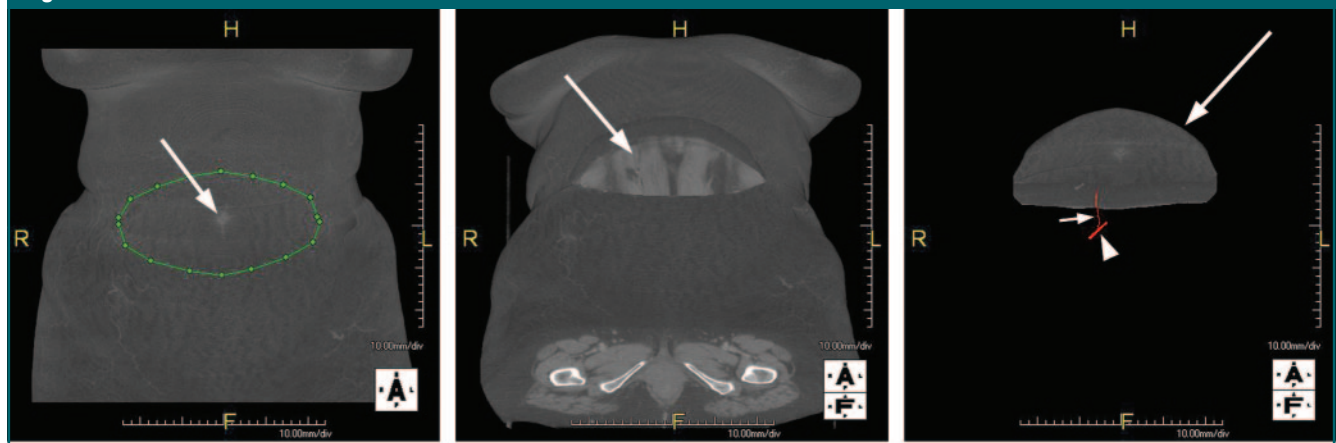


Figure 1: Schematic representations of DIEP flap resection. **(a)** The area of the flap (outlined in green) is centered around the umbilicus (arrow). **(b)** The subcutaneous fat is resected, and the underlying rectus abdominis muscle (arrow) is left intact. **(c)** The flap consists of subcutaneous fat (long arrow), a segment of an IEA (arrowhead), and a perforating branch arising from the IEA (short arrow). Cubes at bottom right are references provided by the workstation to demonstrate exact tilt of the image. A = anterior, F = feet, H = head.

MR Imaging Parameters

Parameter	Value or Description
Sequence	THRIVE
Imaging plane	Axial
Repetition time msec/ echo time msec	4.4/2.2
Flip angle (degrees)	10
Section thickness (mm)	4
Section overlap (mm)	2
Matrix	512 × 384
Z-axis coverage (cm)	16 (Superior edge 5 cm above umbilicus)
Field of view (mm)	320
Voxel size (mm)	0.5 × 0.8 × 2.0
Breath-hold duration (sec)	29

along the axial and craniocaudal axes (in centimeters) were recorded. For each perforator, 3D surface-rendered images of the patient's anterior abdominal wall were generated at a computer workstation (Aquarius, version 1.7.2.19; TeraRecon, San Mateo, Calif). The image postprocessing software of the workstation uses the original 4-mm-thick sections to create 3D volume data. These data can be displayed as a surface-rendered or maximum intensity projection image with a slab thickness of 1 mm or greater. For these examinations, a slab thickness of 1 mm was used during image postprocessing. At the workstation, once an arrow is placed on a maximum intensity projection image, it maintains its position during image manipulations such as change in projection and conversion from maximum inten-

sity projection to surface-rendered image. Thus, once the arrow is placed pointing to the perforator's exit point through the fascia on the axial maximum intensity projection, the maximum intensity projection is changed to a frontal projection and then converted to a surface-rendered image while the arrow's position is preserved. The umbilicus and the points where the marked perforators exited the rectus fascia were marked on the surface-rendered images. The transverse and craniocaudal distances of each perforator from the umbilicus were labeled on a surface-rendered image (Fig 2). The annotated and nonannotated surface-rendered images and the axial images were made available to the surgeons preoperatively.

One perforator on each side of the um-

Figure 2

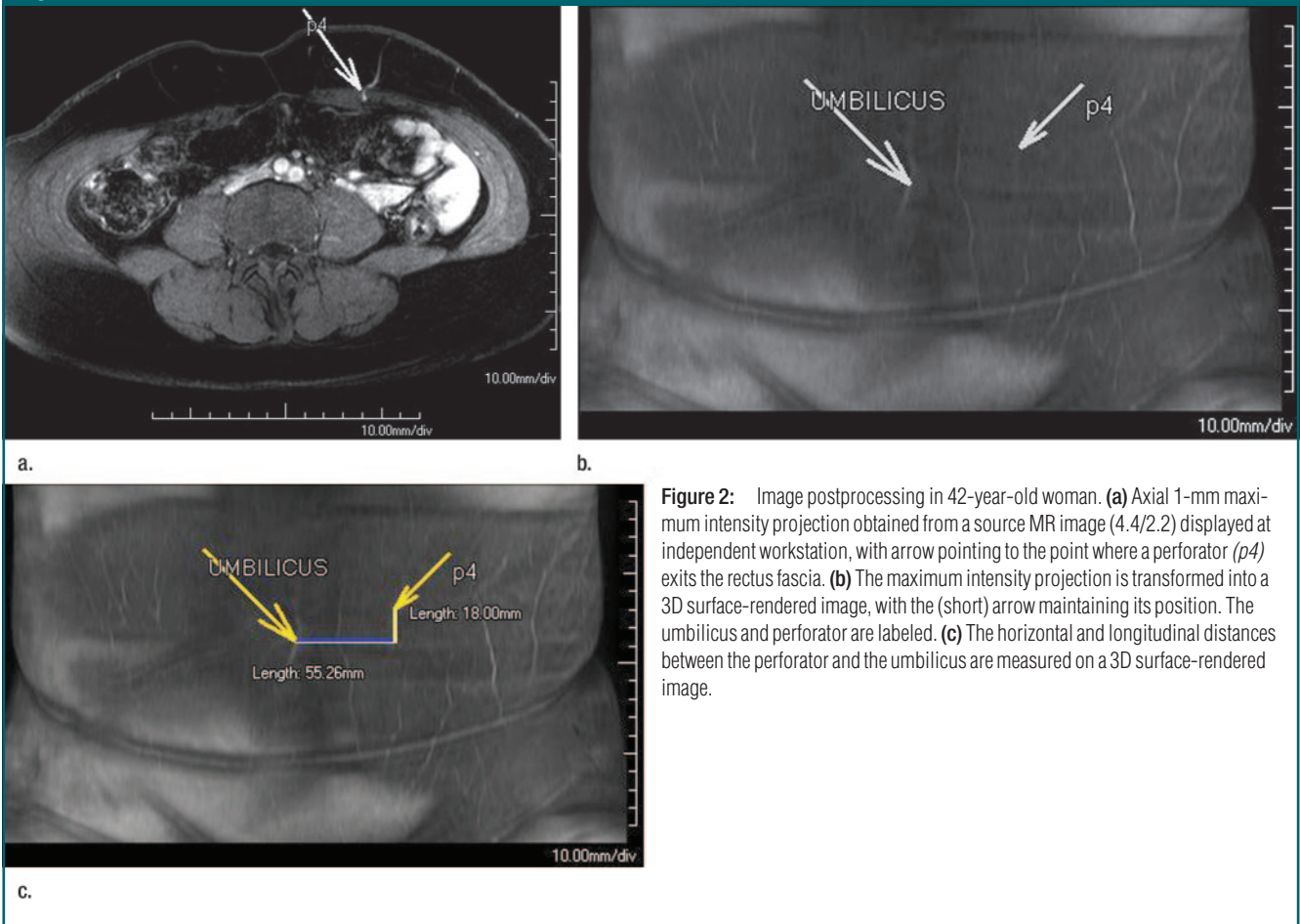


Figure 2: Image postprocessing in 42-year-old woman. (a) Axial 1-mm maximum intensity projection obtained from a source MR image (4.4/2.2) displayed at independent workstation, with arrow pointing to the point where a perforator (*p4*) exits the rectus fascia. (b) The maximum intensity projection is transformed into a 3D surface-rendered image, with the (short) arrow maintaining its position. The umbilicus and perforator are labeled. (c) The horizontal and longitudinal distances between the perforator and the umbilicus are measured on a 3D surface-rendered image.

Figure 3

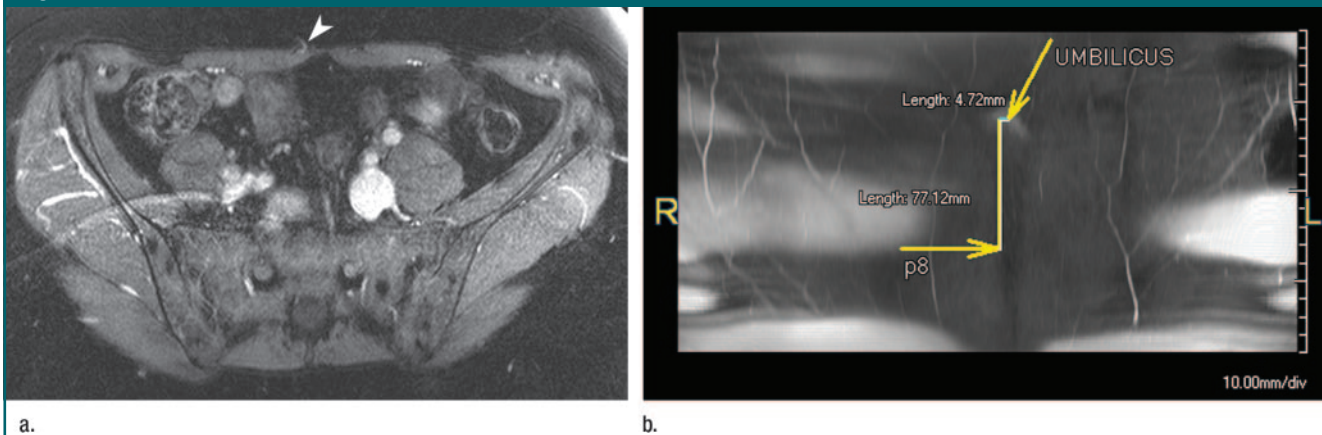


Figure 3: MR images in 50-year-old woman. **(a)** Axial 3D gadolinium-enhanced T1-weighted fat-suppressed gradient-echo MR image (4.4/2.2, 10° flip angle) shows a 1.2-mm perforator (arrowhead) exiting the rectus fascia. **(b)** Three-dimensional surface-rendered image shows a relatively long distance between the perforator (*p8*) and the center of the flap, which is the umbilicus. This perforator was not harvested during surgical dissection owing to its peripheral location.

Figure 4

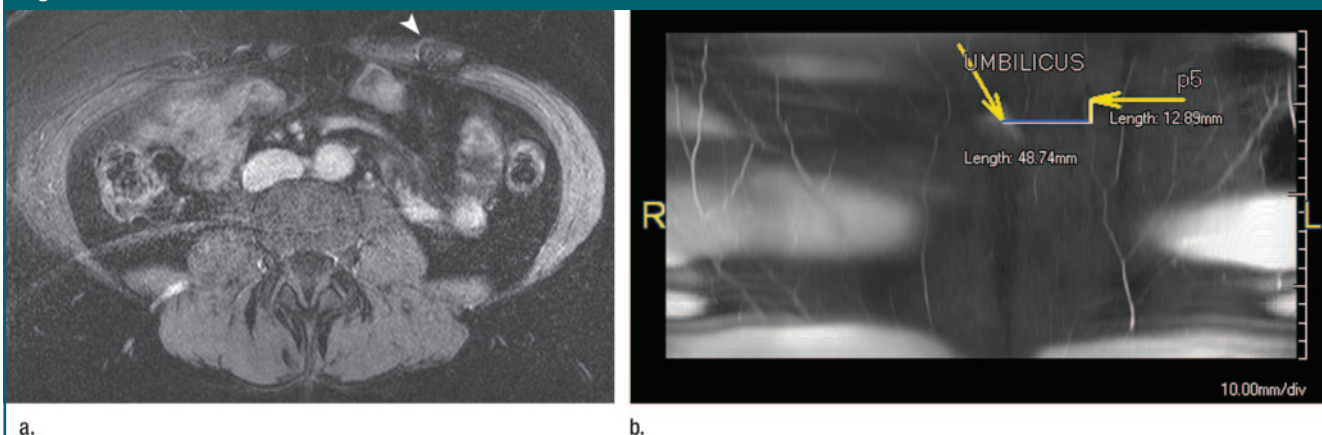


Figure 4: MR images in 50-year-old woman described for Figure 3. **(a)** Axial 3D gadolinium-enhanced T1-weighted fat-suppressed gradient-echo MR image (4.4/2.2, 10° flip angle) shows a 1.3-mm perforator (arrowhead) exiting the rectus fascia. **(b)** Three-dimensional surface-rendered image shows a relatively short distance between the perforator (*p5*) and the center of the flap, which is the umbilicus. This perforator was harvested during surgery owing to its large size and central location.

bilicus was labeled “the best.” The algorithm used to choose the best perforator was based on criteria that our referring surgeons (D.T.G., J.L.L., H.A.E.) use to select the perforator suitable for harvesting intraoperatively. Perforator size was given the highest priority, and in those cases in which a single perforator was the largest, it was labeled as the best. In cases in which there were more than one large perforator equal or nearly equal in size (ie, difference in diameter of not more than 0.1 mm), the perforator located most centrally

with respect to the flap edges (ie, closest to the umbilicus) was labeled as the best. In cases in which there were more than one large perforator equal or nearly equal in size and similarly located with respect to the flap edges, the perforator with the shortest and least tortuous intramuscular course was labeled as the best. The size and location of the perforator were given higher priority over the intramuscular course because perforator size influences flap viability and perforator lo-

cation influences the ease of the surgical dissection (Figs 3, 4).

The patients underwent DIEP flap reconstructive breast surgery performed by a team that consisted of two of the three participating surgeons (D.T.G., J.L.L., H.A.E.), each of whom had 5 years experience in plastic surgery. After DIEP flap reconstructive breast surgery, the preoperative imaging data were compared with the intraoperative findings. Before surgery, the surgeons used the

Figure 5

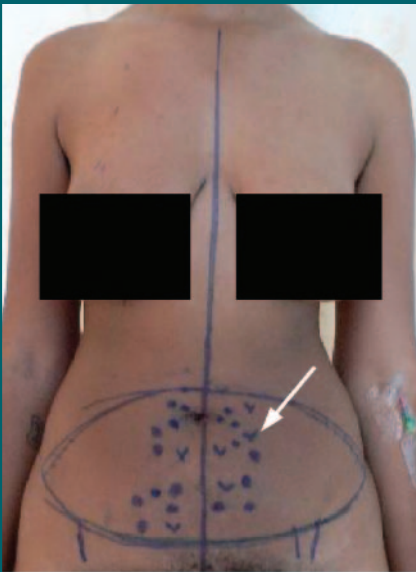


Figure 5: Preoperative markings of perforator locations in anterior abdominal wall on 35-year-old woman. X marks (arrow) correspond to perforator locations identified at preoperative MR imaging. The transverse and craniocaudal distances from the umbilicus to each perforator identified at preoperative MR imaging are used to localize the marks on the patient's skin.

written MR imaging report and the surface-rendered images to translate the points where the perforators exited the rectus fascia, as indicated by the MR report and images, to points on the patient's skin (Fig 5). The skin marks, written MR imaging report, and axial images were used to determine whether the perforators seen on the MR images corresponded to those found intraoperatively. A standardized data sheet was filled out by the surgeon after the surgery. The perforator location on the MR images was considered to be concordant with the intraoperative findings when the distance of the perforator from the umbilicus coincided within 1 cm. This wide range was allowed owing to shifting of the superficial end of the umbilicus as the abdominal wall was being compressed by the MR torso coil (Fig 6).

Statistical Analysis

The mean diameters of all perforators and of the subgroup of perforators labeled as the best were calculated by using SAS, version 9.1.2, software (SAS, Cary, NC) and were compared by using a two-tailed Student *t* test.

P < .05 indicated a significant difference.

Results

After all gadolinium-enhanced acquisition data were analyzed, perforator localization and imaging data postprocessing were performed by using the second gadolinium-enhanced acquisition in 17 (90%) of the 19 patients and the third enhanced acquisition in two (10%). The first gadolinium-enhanced acquisition was not used for interpretation in any patients. No images were excluded because of nondiagnostic image quality.

Preoperative MR imaging depicted a total of 118 perforators, which had a mean diameter of 1.1 mm (range, 0.8–1.6 mm). Thirty perforators were labeled as the best. The mean diameter of the perforators labeled as the best was 1.4 mm (range, 1.0–1.6 mm). The difference between the mean diameter of all perforators and the mean diameter of those labeled as the best was significant (*P* < .0001).

During the surgical dissections, a total of 122 perforators were found, and 33 of these perforators were harvested. Twenty-seven (90%) of 30 flaps were supplied by a single perforator, and three (10%) of 30 flaps were supplied by two perforators. All 118 (100%) perforators seen at preoperative MR imaging were found during surgery. Of the 122 perforators seen intraoperatively, 118 (97%) were localized at preoperative MR imaging. All 33 (100%) of the harvested perforators were seen at preoperative MR imaging. Twenty-eight (85%) of the 33 harvested perforators corresponded to those labeled as the best at preoperative MR imaging. Of the five harvested perforators that were not labeled as the best at MR imaging, three (60%) were in close physical proximity to the one labeled as the best and were harvested as an additional perforator; this resulted in the flap being supplied by two perforators. Two of the five (40%) harvested perforators that were not labeled as the best had diameters that were 0.1- and 0.2-mm smaller than the diameters of the perforators labeled as the best. How-

Figure 6



Figure 6: Axial 3D gadolinium-enhanced T1-weighted fat-suppressed gradient-echo MR image (4.4/2.2, 10° flip angle) in 40-year-old woman shows a superficial end of the umbilicus (short arrow) being shifted to the right relative to the deep end (long arrow) as the surface coil compresses the abdominal wall.

ever, intraoperatively, these two perforators were deemed to have a more favorable location for the patient's anatomy and flap area.

Discussion

Breast cancer is the most common malignancy in women in the United States (6). Although many treatment options exist, mastectomy followed by breast reconstruction remains a popular choice. Although pedicled flap procedures such as TRAM flap reconstruction have been the approaches traditionally used to reconstruct the breast, microsurgical techniques such as DIEP flap reconstruction are gaining popularity (1). Although DIEP flap surgery has certain advantages over TRAM flap reconstruction, such as an improved cosmetic appearance and a decreased rate of complications at the donor site, the tedious search for the small perforators arising from the IEA results in much longer dissection times (1,7). Preoperative knowledge of the location and sizes of IEA perforators would allow the surgeon to avoid scrupulous dissection of the entire flap area and focus on the region where the perforator is expected to pierce the rectus fascia—an approach that requires a much smaller dissection area and, in turn, a shorter dissection time. Preoperative localization of the perforators with cross-sectional imaging has been shown to be effective in reducing the intraoperative time (4,5).

Multidetector CT has been reported to be very accurate in the localization of the perforators (2,4,5). Given that breast reconstruction is a complex cosmetic procedure, one can presume that a younger subgroup of breast cancer patients would seek it; therefore, the additional ionizing radiation exposure associated with CT use might be undesirable. Although the use of traditional preoperative imaging with Doppler US avoids radiation exposure, this examination is operator dependent and is less sensitive and less specific for localization of the perforators compared with CT (2). Furthermore, cross-sectional imaging with CT enables additional information, such as the size and course

of the vessel, to be available preoperatively (2). MR imaging has an advantage over CT in that it does not involve radiation exposure. Our study results demonstrate that MR imaging can be used to accurately map the location of the IEA perforators.

Although multidetector CT yields higher spatial resolution than does MR imaging, MR imaging generally yields greater contrast resolution, which enables the detection of submillimeter gadolinium-enhanced structures such as IEA perforators. Another advantage of MR imaging over CT is that the absence of ionizing radiation allows one to perform multiple acquisitions after the administration of gadolinium-based contrast material. This results in an improved ability to obtain images at the most optimal times—when the signal intensity of the perforators is the highest and venous contamination is the lowest—such that patient-related factors play a lesser role.

We did not use dedicated MR angiography techniques in our study, although such techniques are available for imaging extremely small arteries—for instance, the artery of Adamkiewicz (8,9). The MR angiography techniques described in the Nijenhuis et al (8) and Jaspers et al (9) studies would not be applicable in our series because the spatial resolution in the anterior abdominal wall is unlikely to match that in the region of the spinal arteries. Abdominal wall MR angiography may be further adversely affected by some motion artifact, which is usually present in the abdomen. A spine surface coil could be used to image the abdominal wall; however, using it, compared with using a torso coil, would require prone positioning of the patient in the imaging unit used in our study and would cause a greater degree of distortion of the anterior abdominal wall. In addition, the most important datum for the surgeon is the location at which the perforator exits the rectus abdominis fascia, and we found the axial MR imaging plane to be the most valuable for obtaining such data. Furthermore, performing conventional MR angiography in the axial plane and achieving the desired craniocaudal anatomic

coverage would require an unacceptably long breath hold. Alternatively, axial images can be reformatted from a 3D coronal acquisition. However, the relationship between the rectus fascia and the perforator would not be easily demonstrated with use of either source or reformatted axial MR angiograms.

We chose to use a 3.0-T rather than 1.5-T magnet for this examination because it allows one to achieve the desired spatial resolution and the required craniocaudal anatomic coverage during a single breath hold. Although susceptibility artifact from bowel motion is exaggerated with use of 3.0-T imagers compared with the degree of these artifacts seen with use of 1.5-T imagers, it did not prevent the acquisition of diagnostic-quality images. In addition, the administration of glucagon, although it was not used in our study, may reduce the degree of this artifact. Inhomogeneous fat suppression may be another concern with using 3.0-T imagers; it is particularly problematic in patients with large body habitus. However, this was not encountered in any of the examinations performed in our study. Although patients who are selected to undergo DIEP flap surgery must have some subcutaneous fat for reconstruction of the breast, morbidly obese patients are not candidates for this procedure owing to their increased risk for postoperative complications (7,10). In settings in which a 3.0-T imager is not available, preoperative imaging can be performed with a 1.5-T unit. After completing the data collection for this study, we performed two such examinations by using a 1.5-T imager (data not included). Although the spatial resolution appeared to be lower than that achieved in an average examination performed with the 3.0-T unit, diagnostic image quality was achieved in both cases.

The MR sequence that we used to image the perforators is a 3D T1-weighted fat-suppressed gradient-echo sequence in a volumetric interpolated breath-hold examination (THRIVE). Although a section thickness smaller than 4 mm is achievable with the 3.0-T imager, using this section thickness would

result in a decreased signal-to-noise ratio, which would make detection of the smaller perforators more difficult. In addition, the parameters used in this sequence yield in-plane pixels smaller than 1 mm, allowing the imaging of submillimeter-diameter vessels while keeping the breath hold shorter than 30 seconds. Because the patients selected to undergo DIEP flap reconstruction are relatively young and, aside from having a history of breast cancer, in good health, they generally have no difficulties maintaining a breath hold for the required period.

Identifying the perforators on axial images is fairly straightforward; however, the precise mapping of these vessels in the anterior abdominal wall requires image postprocessing at an independent workstation. We believe that image postprocessing should be performed by a radiologist. There is a learning curve associated with the use of the workstation in these cases; however, once a radiologist becomes proficient in this workstation environment, the entire study interpretation process, including the time spent at the workstation and generating the report, takes about 20–25 minutes.

To plan the dissection, the participating plastic surgeons use 3D images of the patient's anterior abdominal wall as road maps to mark the areas of the perforators on the patient's skin before surgery. Before surgery, the distance of each perforator from the umbilicus in the transverse and craniocaudal directions is determined and is used to

translate the point where the perforator exits the rectus fascia, as depicted on the images, to a point on the patient's skin. The most crucial information for the surgeon is the size of the perforators and the location of a given perforator with respect to the umbilicus. In settings in which an independent workstation is not available, the horizontal and craniocaudal distances between the perforator and the umbilicus can be calculated by using axial MR images and the craniocaudal section locations.

An important limitation of our study was the fact that the effect of the preoperative MR examination on the surgical time was not evaluated. Although anecdotal reports from the participating surgeons suggest that dissection times are greatly reduced, a randomized control study is needed to evaluate the true effect of preoperative MR imaging on dissection times. In summary, a 3D gadolinium-enhanced T1-weighted fat-suppressed gradient-echo sequence performed by using a 3.0-T MR imager can be used to accurately localize IEA perforators and select the most favorable perforator to harvest for DIEP flap reconstructive breast surgery.

References

- Howard MA, Mehrara B. Emerging trends in microsurgical breast reconstruction: deep inferior epigastric artery perforator (DIEP) and the superior gluteal artery perforator (SGAP) flaps. *Int J Surg* 2005;3(1):53–60.
- Rozen WM, Phillips TJ, Ashton MW, Stella DL, Gibson RN, Taylor GI. Preoperative imaging for DIEA perforator flaps: a comparative study of computed tomographic angiography and Doppler ultrasound. *Plast Reconstr Surg* 2008;121(1):9–16.
- Giunta RE, Geisweid A, Feller AM. The value of preoperative Doppler sonography for planning free perforator flaps. *Plast Reconstr Surg* 2000;105(7):2381–2386.
- Alonso-Burgos A, García-Tutor E, Bastarrika G, Cano D, Martínez-Cuesta A, Pina LJ. Preoperative planning of deep inferior epigastric artery perforator flap reconstruction with multisection-CT angiography: imaging findings and initial experience. *J Plast Reconstr Aesthet Surg* 2006;59(6):585–593.
- Masia J, Clavero JA, Larrañaga JR, Alomar X, Pons G, Serret P. Multidetector-row computed tomography in the planning of abdominal perforator flaps. *J Plast Reconstr Aesthet Surg* 2006;59(6):594–599.
- Centers for Disease Control and Prevention (CDC). Decline in breast cancer incidence: United States, 1999–2003. *MMWR Morb Mortal Wkly Rep* 2007;56(22):549–553.
- Vyas RM, Dickinson BP, Fastekjian JH, Watson JP, Dalio AL, Crisera CA. Risk factors for abdominal donor-site morbidity in free flap breast reconstruction. *Plast Reconstr Surg* 2008;121(5):1519–1526.
- Nijenhuis RJ, Mull M, Wilmink JT, Thron AK, Backes WH. MR angiography of the great anterior radiculomedullary artery (Adamkiewicz artery) validated by digital subtraction angiography. *AJNR Am J Neuroradiol* 2006;27(7):1565–1572.
- Jaspers K, Nijenhuis RJ, Backes WH. Differentiation of spinal cord arteries and veins by time-resolved MR angiography. *J Magn Reson Imaging* 2007;26(1):31–40.
- Guerra AB, Metzinger SE, Bidros RS, et al. Bilateral breast reconstruction with the deep inferior epigastric perforator (DIEP) flap: an experience with 280 flaps. *Ann Plast Surg* 2004;52(3):246–252.